Journal of Natural Gas Science and Engineering 25 (2015) 46–57

Contents lists available at ScienceDirect

Journal of Natural Gas Science and Engineering

journal homepage: www.elsevier.com/locate/jngse

Characterization of mineral composition and its influence on microstructure and sorption capacity of coal

Chunmiao Deng [a, b, *], Dazhen Tang [a, b], Shimin Liu [c], Hao Xu [a, b], Shu Tao [a, b]

[a] School of Energy Resources, China University of Geosciences, Beijing 100083, PR China
[b] Coal Reservoir Laboratory of National Engineering Research Center of Coalbed Methane Development & Utilization, Beijing 100083, PR China
[c] Department of Energy and Mineral Engineering, G[3] Center and EMS Energy Institute, The Pennsylvania State University, University Park, PA 16802, USA

ARTICLE INFO

Article history:
Received 5 January 2015
Received in revised form
23 April 2015
Accepted 24 April 2015
Available online 15 May 2015

Keywords:
Mineral occurrence
Mineral composition
Microstructure
Gas sorption capacity
Low rank coal

ABSTRACT

Mineral matter is widely accepts as one of the important factors influencing the gas sorption capacity of coal. By analyzing ash content and Langmuir volume of coals, studies have reported positive, negative, and poor impacts of mineral matter on sorption capacity without convincing reasons explaining the contradictory results. This paper proposes a new analysis method to correlate minerals and gas sorption capacity by connecting the mineral matter compositions to sorption capacity through the variations in the microstructure. In addition to mineral content, mineral occurrence modes and compositions were also studied to investigate their relations with gas sorption capacity.

A total of 22 coal samples are used to interpret the characterization of minerals, including mineral content by proximate analysis, mineral occurrence mode by scanning electron microscope (SEM) and energy-dispersive X-ray spectrometer (EDX) analyses, and mineral compositions by X-ray powder diffraction (XRD) analysis. Low-temperature nitrogen adsorption and high pressure methane adsorption analyses of selected samples are applied to characterize microstructure and gas adsorption capacity.

We found that mineral content, occurrence mode, and composition are three controlling factors that together determined the influence of mineral matter on gas sorption capacity. In fact, some factors have potential for both positive and negative influence. This is why both negative and positive influences have been previously observed. The direction and magnitude of influence depends on the relative weights of the driving factors. For samples in this study, clay mineral content showed the strongest positive relation to S_{BET}, total V_{BJH}, and V_L, compared to total mineral and brittle mineral content. The relation of other minerals to S_{BET}, total V_{BJH}, and V_L is weak. The final result indicated that mineral matter had a positive influence on gas sorption capacity.

1. Introduction

Coalbed Methane (CBM) is labeled as an unconventional natural gas due to its unique storage and flow mechanisms. Gas stored in coal seams occurs dominantly in an adsorbed state on the internal pore surfaces of coal, which can as account for as much as 95% of total gas content (Gray, 1987). Mineral matter is one of the most important factors influencing gas sorption capacity on coals, which also include coal rank, moisture, micro-pore structure, as well as maceral composition and type (Yee et al., 1993; Bustin and Clarkson, 1998).

Various studies have reported that the gas sorption capacity of coal is affected by mineral matter. By comparing ash content to Langmuir Volume, a negative correlation was commonly observed and accepted (Faiz et al., 1992; Yee et al., 1993; Crosdale et al., 1998; Laxminarayana and Crosdale, 1999; Liu et al., 2014; Ma et al., 2014). One interpretation of this effect was that mineral matter has less surface area compared to the microporous organic constituents of coal (Gan et al., 1972; Clarkson and Bustin, 1996). Another interpretation was that the mineral matter was essentially non-adsorbent to methane and acted as a simple diluent to the whole coal matrix (Crosdale et al., 1998; Laxminarayana and Crosdale, 2002). Thus, it was considered as counterintuitive when a positive correlation was found in Australian coals by Bustin (1997). Further, this opposite phenomenon was also found in Black Warrior coals by Carroll and Pashin (2003). On the basis of the

* Corresponding author. School of Energy Resources, China University of Geosciences, Beijing 100083, PR China.
E-mail addresses: chunmiaocugb@gmail.com (C. Deng), szl3@psu.edu (S. Liu).

http://dx.doi.org/10.1016/j.jngse.2015.04.034
1875-5100/

interpretations for a negative relation, it is hard to understand the mechanisms of minerals for enhancing the sorption capacity of coal. In addition, Chalmers and Bustin (2007) reported poor correlation between gas sorption capacity and ash content in subbituminous coals. However, it should be noted that all these studies on the relation between minerals and gas sorption capacity only analyzed the mineral content in relation to gas sorption capacity, and these previous studies ignored the possibility that mineral occurrence and mineral composition may also have impacts on gas sorption capacity.

Studies on mineral occurrence in coal have mainly utilized qualitative analysis, and the studies have been focused on the pore and cleat-fill mineralogy as well as discussing their influence on CBM generation and production (Spears and Caswell, 1986; Daniels et al., 1996; Dai et al., 2006). Diagenetic and epigenetic minerals, such as calcite, pyrite, kaolinite, silica, boehmite, silica, and sphalerite, were commonly filled in cleats (Daniels et al., 1996; Dai et al., 2006). Laubach et al. (1998) and Gamson et al. (1996) concluded that the degree of mineral filling is one of the key factors that retard fluid conduction. Pitman et al. (2003) reported that minerals can affect the gas transmission and storage capacity of Black Warrior coals. Studies on mineral composition have mainly used quantitative analysis, and they have been focused on precisely determining the mineral species and composition ratios as well as discussing the abundance and origin of minerals or trace minerals (Dai and Chou, 2007; Dai et al., 2008; Wang et al., 2012; Liu et al., 2014). Although numerous studies have investigated mineral occurrence and composition, little is known regarding their relationships with gas sorption capacity. Instead, mineral occurrence has been directly correlated to the microstructure of coal. Additionally, the interpretation that mineral material has minimal surface area implicates the microstructure in the relationship between mineral and gas sorption capacity, and this requires further study.

In this study, we primarily analyze the features of mineral material (including mineral content, mineral occurrence, and mineral composition) to elucidate their influence on gas sorption capacity. Qualitative and quantitative analyses are used to reveal the characteristics of mineral occurrence and composition. Attributes of microstructure and gas sorption capacity also are evaluated including surface area, pore structure, Langmuir volume, and Langmuir pressure. Then, we use statistical methods to clarify the relationships among minerals, microstructure, and gas sorption capacity. Finally, we try to explain the contradicting results in the literature regarding the influence of minerals on the gas sorption capacity of coal. This study will lead to a better understanding of the way minerals effects gas sorption capacity, and hence it can act as a foundation for the prediction of gas accumulation and production.

2. Experimental work

2.1. Sample collection and description

A total of 22 coal samples were chosen from five different basins in north China. The samples consisted of large cubic blocks, $30 \times 30 \times 30$ cm^3 in size, were cut from fresh coal faces in active coal mines. Each coal block was carefully sealed with plastic wrap to prevent weathering and oxidation. All the samples were then shipped to the laboratory for experimental tests.

The geographical locations for all 22 samples are shown in Fig. 1 and the detailed information for each sample including location, burial depth, thickness, bearing formations, and rank is shown in Table 1. One sample (A1) was collected from the No. 4 coal seam in the Tuha basin. Three samples (B2, B3, and B4) were obtained from the No. 9 coal seam in the Junggar basin. One sample (C5) was collected from the No. 11 coal seam of the Hailar basin. Two samples (D6 and D7) were selected from the No. 6 and No. 3 coal seam in the northern Ordos basin. Seven samples (D8 to D14) were collected from different coal seams in the western and southern parts of the Ordos basin. Two samples (D15 and D16) were from the No. 11 coal seam of the southeast part of the Ordos basin. The last six samples (E17 to E22) were obtained from the No. 3 coal seam in the southern portion of the Qinshui basin. More details on this five basins, including geological background, CBM exploration status, and the range of coal rank, were investigated from different literature (Liu et al., 2013; Xu et al., 2012; Meng et al., 2014; Li et al., 2014; Su et al., 2005; Cai et al., 2011; Tao et al., 2012; Lv et al., 2012).

2.2. Sample characterization

Proximate analysis was initially performed to set up a baseline for further investigations. The SEM and XRD analyses were then applied to identify, observe, and quantify the mineral matter. Based on prior results, fourteen samples were selected for low-temperature nitrogen (N_2) adsorption to characterize the surface area and pore structure. Finally, sorption isotherms were estimated to quantify the gas sorption capacity. To minimize oxidation, all the crushed samples were stored in environmental chambers and maintained at temperatures less than 10 °C.

2.2.1. Proximate analysis

A 5E-MAC III infrared fast coal analyzer was used to determine the moisture, volatile matter, ash yield, and fixed carbon content of 22 coal samples. The tests were performed in accordance with standard procedures (ASTM, 2006) at the National Engineering Research Center of CBM Development & Utilization at the China University of Geosciences, Beijing.

2.2.2. SEM and XRD tests

Two or three small pieces were cut from each of the 22 coal samples so that each piece had one face with an area of approximately 1×1 cm^2. These subsamples were used for SEM and EDX analyses at the laboratory of the National CBM Engineering Research Center in China. The accelerating voltage was 20 KV and the beam current was 10^{-10} A.

The remaining material of the 22 coal samples were pulverized down below 200 mesh for XRD analysis with a LabX XRD-6000 at the laboratory in National CBM Engineering Research Center in China. Samples were scanned from 5 to 45° 2θ, with a step interval of 0.04 s and a 2 s counting time for each step. The X-ray diffractograms of 22 samples were subjected to quantitative mineralogical analysis using Siroquant™. This commercial interpretation software was developed by Taylor (1991) using the principles of diffractogram profiling explained by Rietveld (1969). Further details demonstrating the use of this technique for coal-related materials are given by Ward et al. (1999, 2001) and Ward (2002).

2.2.3. Low temperature N_2 isotherm measurements

The 14 samples chosen for further testing were pulverized to 100 mesh. The N_2 low-temperature (77 K) adsorption/desorption tests were performed following the Chinese National Standard (GB/T19587, 2004) via a Quadrasorb SI analyzer. The Brunauer, Emmett, and Teller (BET) method was used to indicate the specific surface area from the nitrogen isotherm data (Brunauer et al., 1938). The BET equation is expressed as:

$$\frac{1}{W\left(\frac{P_o}{P}-1\right)} = \frac{1}{W_m C} + \frac{(C-1)}{W_m C}\left(\frac{P}{P_o}\right) \quad (1)$$

where, W is the weight of gas adsorbed at pressure P, W_m is the

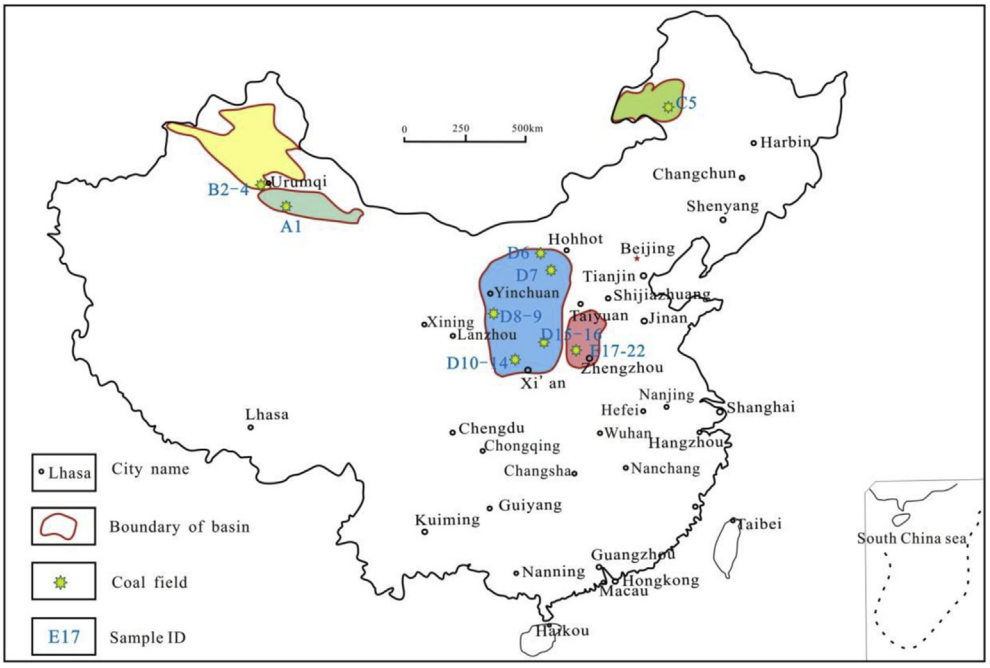

Fig. 1. Location of 22 coal samples from five basins, including Tuha basin (A1), Junggar basin (B2–B4), Hailar basin (C5), Ordos basin (D6–D16), and Qinshui basin (E17-E22).

weight of gas adsorbed as monolayer, C is a BET constant, and P/P_o is the relative pressure of adsorbate.

The Barrett, Joyner, and Halenda (BJH) theoretical framework (1951) was based on the BET multilayer adsorption theory and capillary condensation of vapors in the porous material. The N_2 adsorption isotherms were measured for relative pressures ranging from 0.01 to 1 to obtain pore BET surface area (S_{BET}), BJH pore volumes (V_{BJH}), and the pore size distributions.

2.2.4. Methane isotherm measurements

High-pressure methane isotherms were obtained by a static volumetric adsorption apparatus similar to designs reported by many researchers (Pillalamarry et al., 2011). Eight samples were chosen, pulverized, and sieved to obtain a desired size of 40–100 mesh. To achieve moisture equilibrium, prepared samples were placed in an environmental chamber for more than 48 h at reservoir temperature (23 °C) and humid conditions (99%).

Before starting the experiment, the void volume of the sample container was estimated by helium expansion. The methane was then injected in step-wise manner to the reference cell, and subsequently the valve between the reference cell and sample cell was opened to allow gas to flow into sample cell. A high resolution data acquisition system (DAS) was used to record the pressure data at half-hour intervals. When the pressure readings were constant and identical in both reference and sample cells for a period of more than 2 h, it was believed that the sorption equilibrium had been reached. This normally took 24 h for each pressure step and total pressure changed in a range of 0.2–6.5Mpa. The water bath temperature was 23 °C for this methane isotherms measurement.

The Langmuir sorption model was employed to describe the sorption capacity (Langmuir, 1918). The equation is given as:

$$V = \frac{PV_L}{P + P_L} \tag{2}$$

where, P is the equilibrium gas pressure, V is the volume of gas adsorbed, V_L is the Langmuir Volume representing the maximum volume that can be sorbed at infinite pressure, and P_L is the Langmuir Pressure at which the sorbed volume is half the Langmuir Volume.

3. Results and discussion

3.1. Mineral content in coal by proximate analysis

Coal samples vary markedly in their moisture, fixed carbon (Fix C), ash, and volatile matter (VM), and therefore they can exhibit a wide range of compositions. Based on the coal rank shown in Table 1, all samples can be divided into two major groups: a low rank group with R_o values less than 0.7% and a middle–high rank group with R_o values more than 1.6% (Fig. 2). The low rank group corresponds to lignitic sub-bituminous coals with carbon contents ranging approximately from 51.75% to 73.62%. These coals are enriched in moisture (air dry basis) and volatile matter (dry basis)

Table 1
Basic information for coal samples.

Basin	Sample ID	Period	Formation	Coal thickness (m)	Depth (m)	R_o (%)
Tuha	A1	Mid-Jurassic	Xi shanyao	3.17–12.82	300	0.45–0.55
Junggar	B2–B4	Mid-Jurassic	Xi shanyao	28.01–38.83	225–270	0.38–0.82
Hailar	C5	Low-Cretaceous	Yi min	0.53–13.76	290	<0.5
Ordos	D6–D16	Pennsylvanian	Tai yuan	1.62–36.80	180–724	0.45–1.68
		Jurassic	Yan an	0.28–30.56	190–700	0.41–0.52
Qinshui	E17–E22	Low-Permian	Shan xi	2.20–8.75	350–680	2.2–4.5

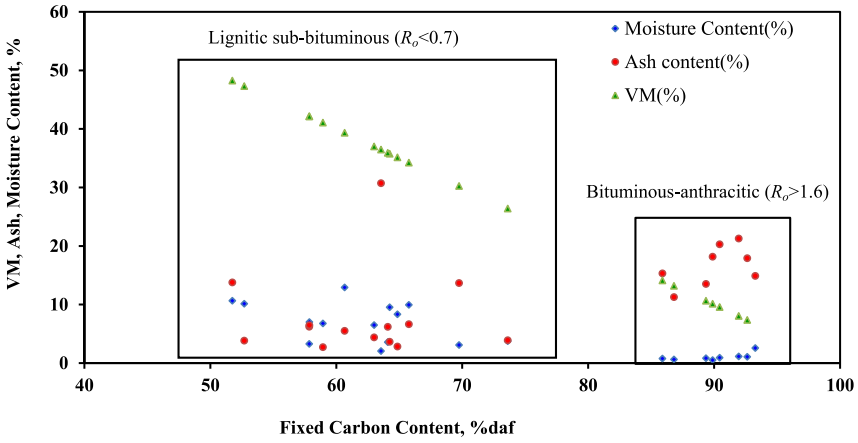

Fig. 2. Proximate analysis data showing the fixed carbon content in relation to moisture, ash, and volatile matter content.

which vary from 2.05 to 10.63 wt% and 26.38 to 48.25 wt%, respectively. The middle–high rank group corresponds to bituminous-anthracitic coals with approximate carbon contents ranging from 85.90% to 93.27%. These coals have extremely low moisture content but relatively high ash content, ranging from 0.51 to 2.55 wt% and 11.25 to 21.27 wt%, respectively. Although coalbed methane production in China is currently almost exclusively from middle–high rank coal, the potential of low rank coal is considerable. More efforts are needed to successfully explore and develop low rank coal. Considering the wide range of R_o in middle–high rank coal, this paper focuses on the low rank coal when comparing minerals and gas sorption capacity in order to mitigate the influence of R_o.

3.2. Mineral occurrence by qualitative analysis

3.2.1. Mineral identification

SEM analysis was performed to observe minerals and their occurrence modes in all coal samples. Numerous well-crystallized or particularly shaped mineral particles and aggregates were easily observed (Fig. 3). Vermicular and platy aggregates of kaolinite were the most commonly observed minerals in the samples (Fig. 3a and b). Calcite was also widely observed in samples with some exhibiting aggregated and fibrous morphologies (Fig. 3c) and a few instances of vein calcite (Fig. 3d). Spherical or granular shaped quartz was also typically observed in coal samples (Fig. 3e and f). Using EDX analysis, some mineral species can be identified by quantifying their element composition ratios. As shown in the rectangle section of Fig. 4a, only fibrous calcite was easily identified by its specific morphology. However, pyrite was recognized according to the EDX analysis result of this selected area shown in Fig. 4b.

3.2.2. Mineral occurrence modes

Distributed on surface of matrix, filled in fractures, and filled in pores are three typical occurrence modes of minerals in coal. Minerals with well-developed morphologies were mainly observed on the matrix surface in all coal samples, which decreases the chance of contact between gas and porous organic constituents (Fig. 3a, b, c, and e). This indicates a negative influence of minerals on gas sorption capacity. However, the degree of this negative influence may be mitigated by the many interspaces that were formed between crystallized minerals and aggregations which may provide paths for gas flowing to the coal matrix.

Mineral infillings observed in micro-fractures and pores were mainly non-crystalline mineral detritus (Fig. 4c, d, e, and f) and a few well-developed crystalline minerals (Fig. 3d and f). Cell cavities of telinite and fusinite with diameter ranges from 5 to 10 μm were preferred spaces for infillings, especially in low rank coals. Fig. 4c shows mineral infillings in a cross section of fusinite, and Fig. 4d shows a vertical section. On the telocollinite, detritus was commonly observed in pores with diameters varying from 1 to 5 μm (Fig. 4e). Micro-fractures with aperture sizes ranging from 0.5 to 8 μm were widespread in coals and also were favored spaces for infillings (Fig. 4f).

In general, minerals that fill or partially fill gaps are undesirable for gas sorption capacity because they decrease the pore volume and internal surface area. However, we found evidence that may support an opposite impact of mineral infillings on gas sorption capacity. As shown in the rectangle in Fig. 4f, micro-fractures are more likely to develop due to the stimulation of the mineral infilling, and these micro-fractures have significant potential for connecting the pores to the primary fracture. In fact, this suggests that mineral infillings could possibly change the effective gas transportation path to some degree. Besides, a study has shown that most of the fractures and macropores, even filled with minerals, are more permeable to gas flow than coal matrix and therefore constitute preferential pathways (Karacan and Okandan, 1999). Furthermore, minerals may be advantageous for gas sorption in coal if they connect some dead end pores.

3.3. Mineral composition by quantitative analysis

Traditionally, the low temperature ash (LTA) of coal was initially obtained to eliminate the organic matter effects on the XRD analysis, and then LTA was used for XRD scanning. However, with the advancement of XRD technology, it is now possible to directly scan the raw coal for determination of major/minor mineral phases (Koukouzas et al., 2010). Some researchers began to compare the results between LTA and direct scanning, and they found that LTA always generates secondary by-products and dehydrated minerals such as bassanite from gypsum and liberated Ca and SO_2, dehydrated clays, and partial destruction of pyrite (Ward, 2002; Koukouzas et al., 2010). In addition, the processing times of LTA are slow (1–2 weeks), especially for low rank coals. Therefore, we chose to perform the XRD measurements with raw coal samples for this study.

The mineral species and composition ratios in coal samples are presented in Table 2. It was more reasonable to analyze the mineral composition by mineral groups, because of the different classes of

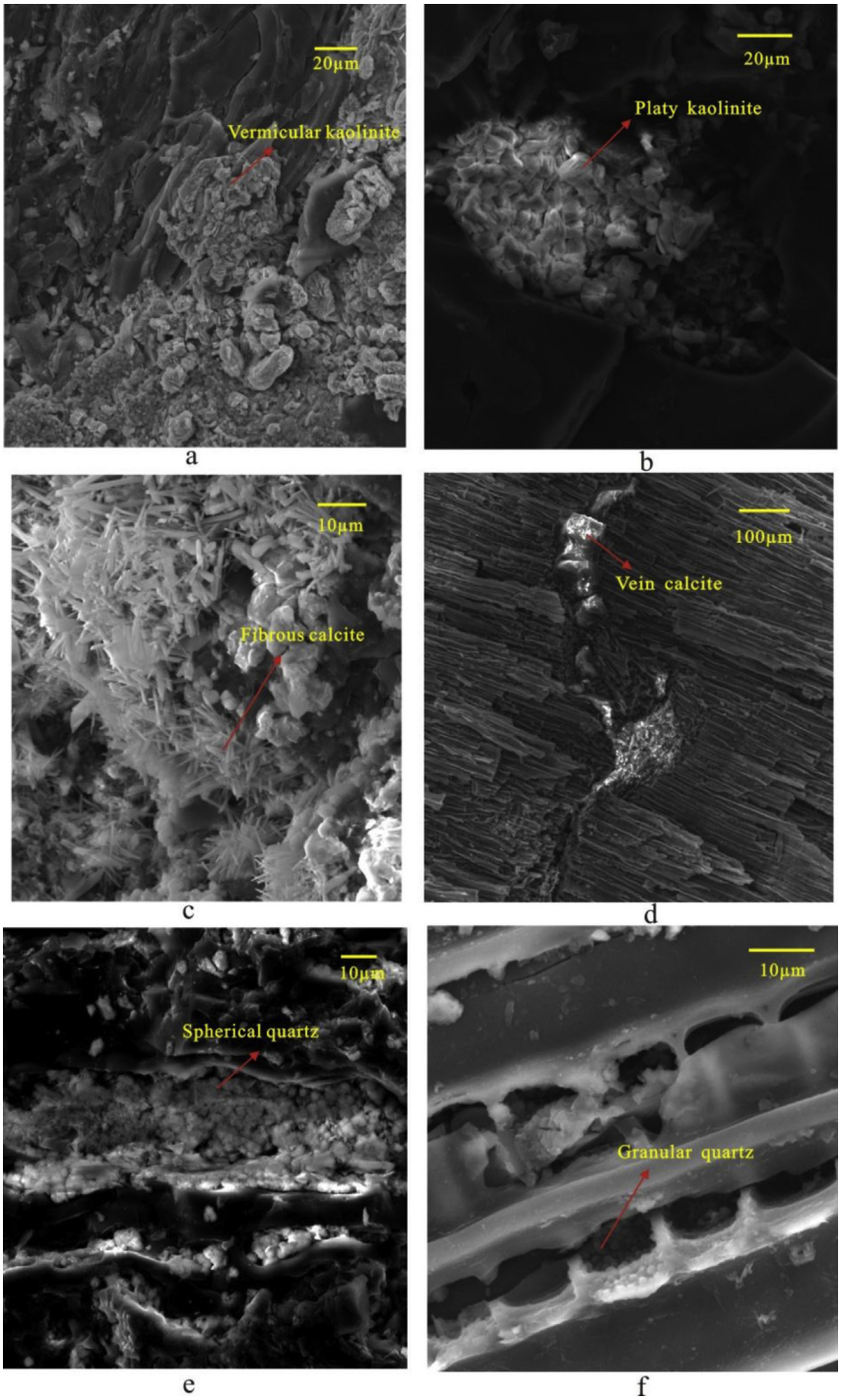

Fig. 3. SEM images showing well crystallized minerals dispersed on matrix surface and within pores and micro-fractures. a: vermicular kaolinite on matrix surface, b: platy kaolinite on matrix surface, c: fibrous calcite on matrix surface, d: vein calcite in micro-fracture, e: spherical quartz on matrix, f: granular quartz in pore.

mineral species observed in coal. These minerals are mainly clay minerals and to a lesser extent carbonates, sulfides, sulfates, and quartz. Phosphates and other mineral species occur more rarely. To better illustrate the distribution of mineral compositions in coal, six mineral groups were designated and plotted in Fig. 5.

The clay mineral group comprises the main minerals in all types of coal. Clay minerals typically account for over 50% of total minerals and can approach 90% in some cases. Kaolinite is the most widespread mineral according to SEM and EDX analyses, occurring mainly as dispersed inclusions on the surface of maceral. Clay minerals have non-negligible surface area which could adsorb gas to some degree (Chen and Huang, 2004). In addition, Zhang et al. (2010) reported higher clay content in a coal reservoir with higher BET surface area.

The minerals in the carbonate group are the second most abundant in samples, generally accounting for over 10% of the total with a maximum of 40%. In this group, calcite and dolomite are widespread in low rank coals, aragonite is common in high rank coals, and siderite is fairly abundant in both coals. Calcite frequently occurs in veins or as well-crystallized aggregates.

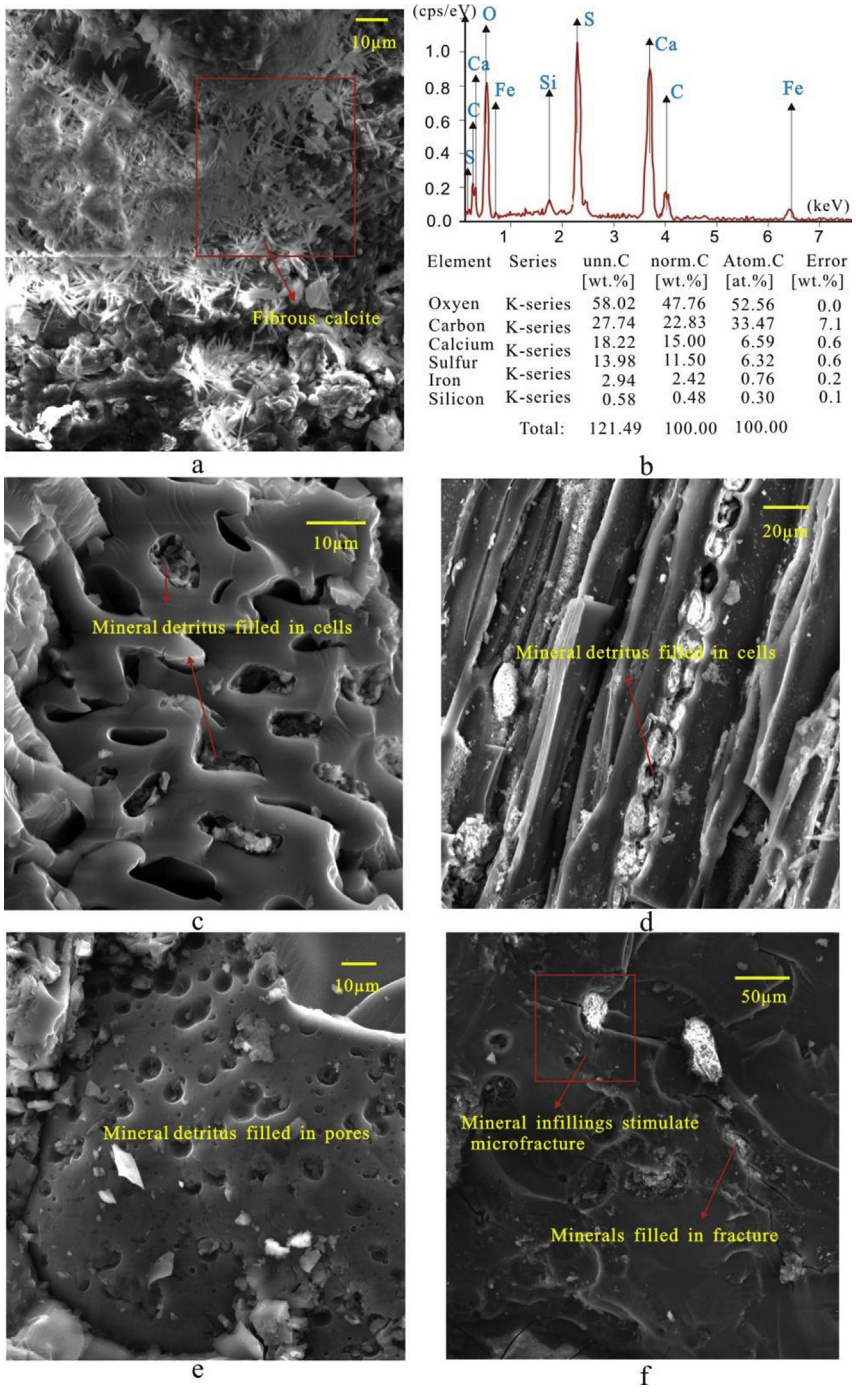

Fig. 4. SEM and EDX analysis showing specific mineral identification and mineral occurrence modes in coals, a: fibrous calcite in the rectangle section, b: EDX analysis result of the rectangle section, c: mineral detritus filled in cells, d: mineral detritus filled in cells, e: mineral detritus filled in pores, f: minerals filled in fracture, and mineral infillings stimulate micro-fracture.

Sulfide minerals are the third most abundant in high rank coal samples, normally making up approximately 6% of the total with the maximum at 15%. Pyrite and marcasite are the most common sulfide minerals, and they occur as veins, cleat coatings, and infillings or replacements of some plant textures.

Sulfate minerals and quartz are the third most abundant minerals in low rank coals. Sulfate minerals can be detected in 40% of the low rank coal samples with contents ranging from 4 to 25%. Gypsum is the most widespread of the sulfate minerals. Quartz can be detected in 70% of the low rank coal samples with content ranging from 3.9 to 46.1%. Quartz in coal has different states and shapes, such as euhedral crystals, nodules, framboids, veins, cleat coatings, and infillings or replacements of some plant textures.

Although most minerals have no potential to adsorb gas, some minerals possess relatively high hardness and brittleness such as carbonate minerals and quartz. Strong minerals deposited within fractures could keep them open, hence may have potential to increase the rate of gas flow (Stowell et al., 2001). Karacan and Okandan (1999, 2001) also mentioned that strong minerals filled in fractures did little harm to gas flow.

Table 2
Mineral composition of raw coal samples by XRD analysis (%).

Minerals	Low rank													Middle-high rank								
	A1	B2	B3	B4	C5	D6	D7	D8	D9	D10	D11	D12	D13	D14	D15	D16	E17	E18	E19	E20	E21	E22
Clay group	41.7	65.2	65.4	63	50.8	58.6	56.8	50.9	58.7	45.2	14.5	57.6	66.7	40.7	66.7	48.6	78.1	53.6	79.6	63.7	62.8	89.2
Quartz				7.8	46.1	3.9	11.3	5.4			12.4	27.6	7.8	10.8			1.5		1.3		2.5	
Plagioclase									7.6				5.1					2.7	2.9	1.6	3.9	
k-feldspar							3.3														3.8	
Calcite		3.0		1.1	3.1	14.4		15.3	13.3		44.4	14.8	16.6	38.5	4.8	43.9						
Dolomite	58.3	15.9		0.8							24.6						6.4	8.6		5.5		
Aragonite																		17.5	10.1	16.3	17.2	
Hematite				5.6				4.0		14.4												
Magnesite		4.1	6.6	7.9		14.4								1.3								
Siderite			2.9	13.8		3.2		14.1	5.7	1.8				5.6			3.4	11.2		1.1	2.0	3.4
Pyrite											4.1			3.1		7.5		6.4				4.6
Marcasite							14.3								17.2		6.4		6.1	5.1	7.8	
Dawsonite										38.6			3.8							2.5		
Diaspore									8.8											1.4		2.8
Boehmite		7.8																				
Barite							9.4								11.3		4.2					
Analcime			14.8			5.5																
Plaster			10.3				4.9	10.3	3.8													
Gypsum		4.0							2.1											2.8		

3.4. Effect of minerals on microstructure and gas sorption capacity of coal

3.4.1. Mineral in relation to microstructure of coal

In the previous sections, we studied characteristics of minerals occurrence and composition, and discussed their relation to microstructure. Minerals on the matrix surface or in pores and fractures decreased the surface area, furthermore, mineral infillings also decreased the pore volume. However, some interspaces between minerals and the stimulation of new micro-fractures may increase flow network connectivity and could even connect some dead end pores to increase surface area and pore volume. Additionally, clay minerals have notable surface area. Thus, the surface area and pore volume of coal need to be evaluated to reveal their relationships with minerals.

Table 3 shows the microstructure parameters of 14 coal samples including S_{BET}, total V_{BJH}, average pore diameter, and pore size distribution. S_{BET} ranges from 0.124 to 34.2 m^2/g, and the total V_{BJH} ranges from 0.001 to 0.028 ml/g Fig. 6 shows the relation between minerals and microstructure by plotting the values of S_{BET} and total V_{BJH} as a function of mineral content and composition. Total mineral content was represented by ash content, and mineral compositions were quantified by clay minerals and brittle mineral (quartz). The method for calculating the content of mineral composition was multiplying the ash content by the ratio of minerals from XRD results.

Both the S_{BET} and total V_{BJH} follow an increasing trend with the increasing of total minerals, clay minerals, and brittle minerals. This result indicates that the positive influence of minerals on the microstructure of these coal samples weighs larger than the negative influence. The positive correlations between minerals and total V_{BJH} are apparently better than the ones between minerals and S_{BET}, which suggests that minerals have a larger influence on total V_{BJH} than on S_{BET}. The correlations in of clay minerals with S_{BET} and total V_{BJH} are the best. This result supports the former points that clay minerals have notable surface area and that there are increasing interspaces among mineral aggregates of well-developed morphologies. It also infers that clay minerals have significant influence on microstructure. Fig. 6d and f shows that there is no noticeable trend between brittle minerals and S_{BET} and that there is an acceptable positive relation between brittle minerals and total V_{BJH}. This result agrees with the previous explanation that strong minerals benefit from the connectivity of micropores and fractures of coal.

3.4.2. Microstructure in relation to gas sorption capacity of coal

Minimal or none existent surface area for gas adsorption is the important and commonly accepted explanation for the negative influence of minerals. However, there is almost no research to support this explanation that quantitatively analyzes how microstructure mediates the effect of minerals on gas sorption. Hence, our aim is to establish the correlation between microstructure and gas sorption capacity via quantitative analysis.

We selected 8 coal samples with similar coal rank

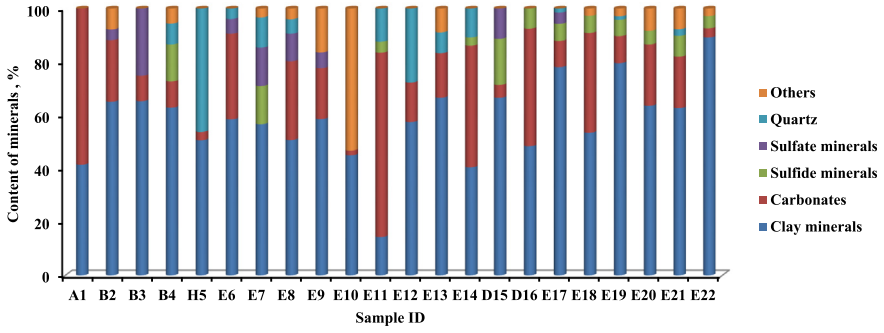

Fig. 5. Groups of mineral composition content histogram, including groups of clay minerals, carbonates, sulfide minerals, sulfate minerals, quartz, and others.

Table 3
Test results of microstructure and gas sorption capacity parameters along with summary information of mineral content.

Sample ID	S_{BET} (m^2/g)	V_{BJH} (ml/g)	Average pore diameter (nm)	Pores proportions (vol. %)			Types of isotherms	P_L	V_L	Ash content	Clay minerals content	Brittle minerals content
				Rmac	Rmeso	Rmic						
A1	0.124	0.002	38.30	0	93.60	6.31	C	6.43	10.98	6.21	2.59	3.62
B2	8.792	0.005	6.12	13.92	16.78	69.30						
B3	1.098	0.001	5.94	27.58	17.27	55.16	A	6.92	9.96	4.39	2.87	0.00
B4	2.168	0.002	6.46	0	35.96	65.04						
D6	34.200	0.025	4.18	1.33	6.18	92.40	A	2.85	13.65	12.9	7.56	2.36
D7	1.283	0.004	10.13	22.83	41.93	35.24	B	6.91	8.58	3.82	2.17	0.43
D8	1.544	0.004	14.18	29.80	45.06	25.14	B	6.22	9.43	3.63	1.85	0.20
D9	1.015	0.003	15.33	36.10	43.15	20.74	B	6.23	11.54	6.63	3.89	0.00
D10	10.918	0.008	5.48	11.70	12.84	75.46						
D11	20.552	0.020	4.63	0	15.07	84.93	A	5.84	13.39	30.71	4.45	25.00
D13	9.930	0.014	5.96	0	28.63	71.37	A	4.95	18.15	6.19	4.13	1.83
D14	12.853	0.018	6.78	9.71	29.30	60.99						

($R_o = 0.45–0.58$, carbon content 52.70–65.77%) and widely varying ash content (3.63–30.71%) for the methane isotherm sorption testing. To better reveal the relation between microstructure and gas sorption capacity, the results are presented in Table 3 along with other summary information including microstructure parameters. The V_L of the 8 samples ranges from 8.58 to 18.15 ml/g, and the P_L varies from 2.85 to 6.92 MPa. Average pore size varies from approximately 4 to 38 nm, and the pore size distribution is subdivided into micropores with pore diameters less than 10 nm, mesopores with diameters from 10 to 100 nm, and macropores with diameters more than 100 nm.

Based on the features of N_2 adsorption isotherm curves, which indicates the geometry of pores, three typical types were distinguished according to the classification of isotherms by Yao et al. (2008). For further information, Liu et al. (2009) compared this classification to the more commonly used IUPAC six isotherm types and four hysteresis loops.

Four samples were classified as type A, and three of them have high sorption capacity and low average pore size. The relatively low sorption capacity of the one sample is due to its low micropore ratio, surface area, and pore volume (Table 3). Sample D13 with the highest sorption capacity is representative of type A isotherms. Its isotherm curve and pore size distribution are shown in Fig. 7, illustrating the commonly developed, well-connected, and ink-

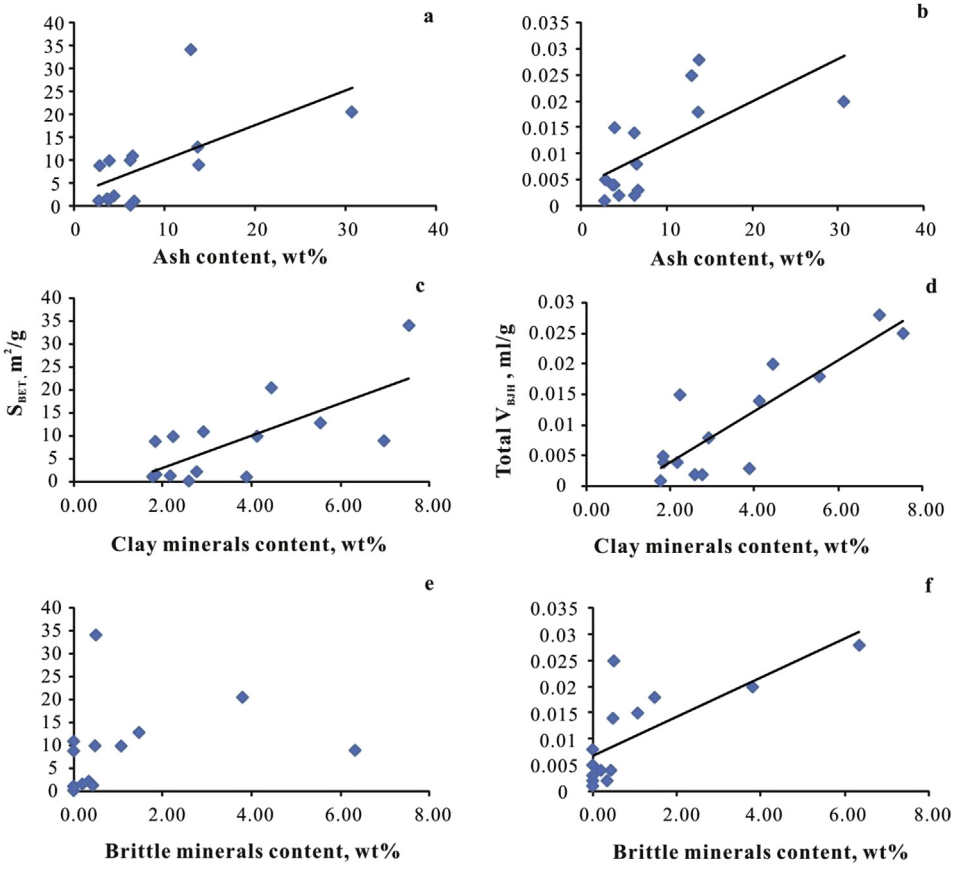

Fig. 6. Relationships between three types of mineral group and microstructure, a: relationship between total minerals (represented by ash content) and S_{BET} (BET surface area); b: relationship between total minerals and total V_{BJH} (BJH volume); c: relationship between clay minerals and S_{BET}; d: relationship between clay minerals and total V_{BJH}; e: relationship between brittle minerals and S_{BET}; f: relationship between brittle minerals and total V_{BJH}.

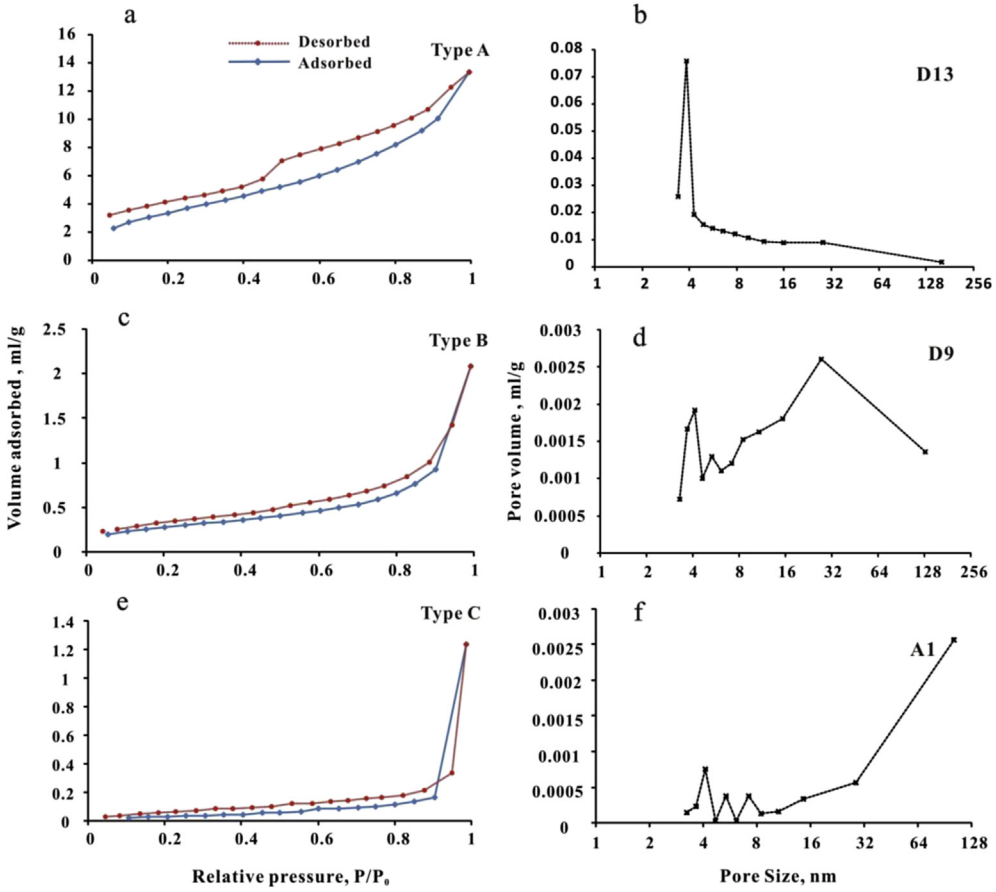

Fig. 7. Low temperature N_2 isotherm types and pore size distribution, a: typical type A isotherm curve (represented by sample D13); b: pore size distribution of D13; c: typical type B isotherm curve (represented by sample D9); d: pore size distribution of D9; e: typical type C isotherm curve (represented by sample A1); f: pore size distribution of A1.

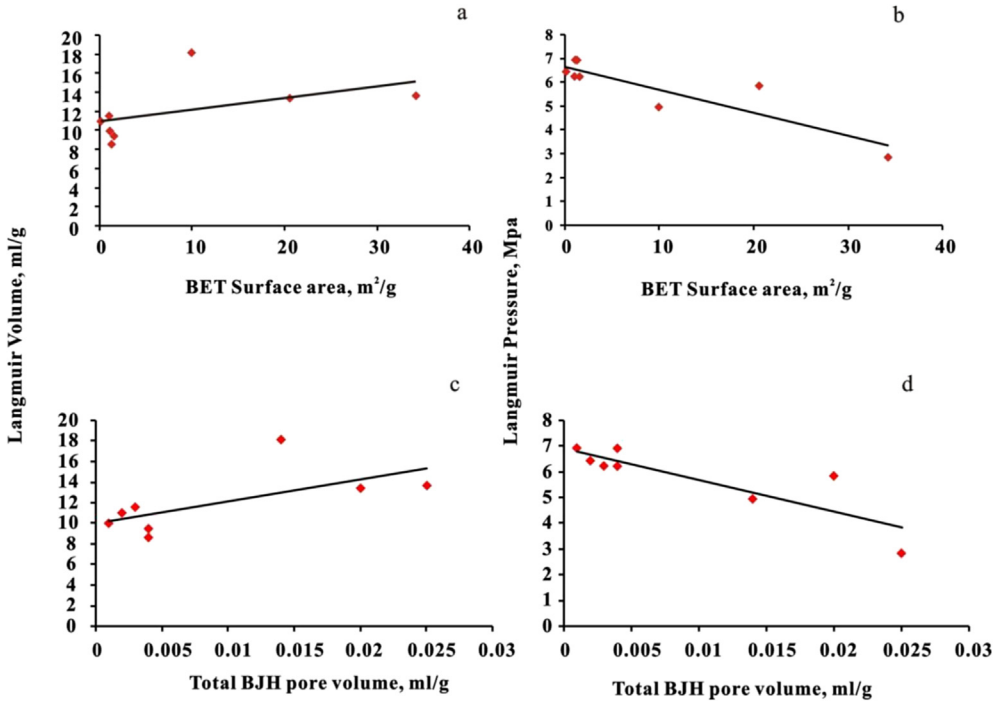

Fig. 8. Relationships between microstructure and gas sorption capacity, a: relationship between BET surface area (S_{BET}) and Langmuir volume (V_L); b: relationship between S_{BET} and Langmuir pressure (P_L); c: relationship between total BJH pore volume (V_{BJH}) and V_L; d: relationship between total V_{BJH} and P_L.

bottle shaped morphology of micro- and mesopores. The hysteresis hoop represents the capillary condensation of nitrogen taking place at P/P_o = 0.45–0.52, which corresponds to a pore diameter of approximately 4 nm.

Three samples are classified into type B, which is represented by D9 (Fig. 7). These coals have a higher ratio of meso- and macropores with an average pore size of 10 nm, generally well-developed mesopores with narrow slitshaped morphology, and good interconnectivity. It is easy to identify three pore volume distribution peaks. Two of the peaks are at ~4 and ~30 nm, and there is a minor peak at ~5 nm. Type B is characterized by the adsorption/desorption curves slowly growing at lower P/P_o but increasing rapidly when P/P_o is more than 0.9.

Type C is similar to type B in the configuration of isotherm curves, but the adsorption amount grows at an insignificant rate when P/P_o is less than 0.9. Type C isotherms commonly represent poorly connected, semi-sealed, and narrow tubular mesopores. Sample A1 is representative of type C isotherms. Micropores less than 10 nm in diameter make up a negligible ratio of its volume, and its highest pore volume peak is at approximately 128 nm (Fig. 7). Both type B and C samples have relatively low gas sorption capacity, and this is due to many factors such as low mircropore ratio, low surface area, low pore volume, and high average pore size.

Fig. 8 shows a positive correlation between methane adsorption capacity (V_L) and surface area but a negative correlation between Langmuir pressure and surface area. Similar correlations occur between total pore volume and these two parameters (V_L and P_L). The increased surface area and pore volume increase the amount of sorption sites and enhance gas sorption capacity. Decreasing P_L with increasing surface area and pore volume illustrates that larger surface areas and pore volumes increase the speed of adsorption saturation.

3.4.3. Mineral composition in relation to gas sorption capacity of coal

There are no noticeable trends found when comparing sorption capacity with total minerals and brittle minerals (Table 3). This indicates that minerals have a complex influence on gas sorption capacity that is not only determined by the mineral content but also by the mineral composition and mineral occurrence. Unfortunately, it is hard to quantify the influence of mineral occurrence on gas sorption capacity. In fact, poor trend between minerals and gas sorption capacity in low rank coals has been reported before (Chalmers and Bustin, 2007).

However, a fair positive trend could be observed after excluding sample D11, which has extremely high ash content (Fig. 9a and c). In Fig. 9b, a better positive correlation between clay minerals and gas sorption capacity can be found even without eliminating that abnormal sample. This is reasonable because clay minerals also have a better correlation with microstructure than the other two types of minerals (Fig. 6). Correlations of clay minerals with V_L and P_L are also the best (Fig. 9), which suggests that clay minerals have a significant influence on gas sorption capacity.

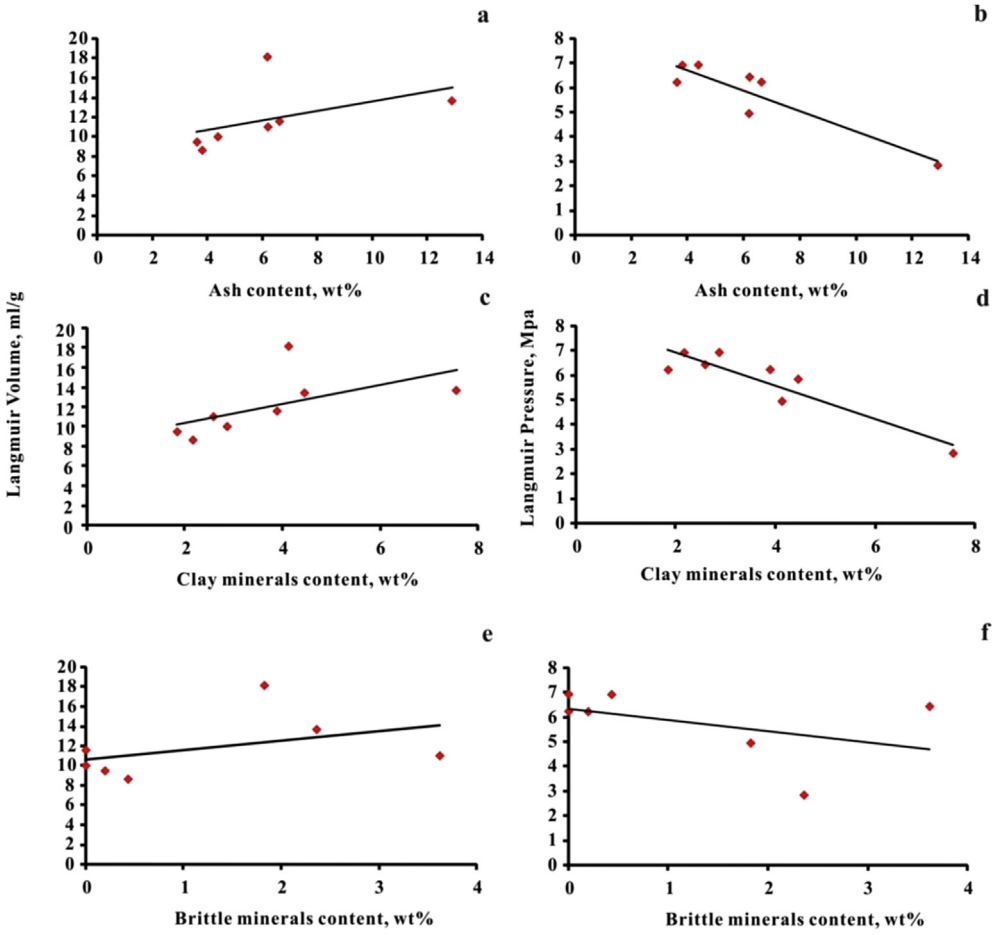

Fig. 9. Relationships between three types of mineral group and gas sorption capacity, a: relationship between total minerals and V_L; b: relationship between total minerals and P_L; c: relationship between clay minerals and V_L; d: relationship between clay minerals and P_L; e: relationship between brittle minerals and V_L; f: relationship between brittle minerals and P_L.

The negative correlation between minerals and V_L is similar to the relationship between microstructure and V_L (Figs. 9b, d, f and 8b, d). This performance indicates that minerals may also have the potential to enhance the gas sorption speed.

Furthermore, all three types of minerals have more notable positive trends with microstructure than with gas sorption capacity (Figs. 6 and 9). The relatively weak correlation between microstructure and gas sorption capacity can be seen in Fig. 8. This represents a decreased degree of influence compared to that of minerals on microstructure. This agrees with the statement that microstructure served as a middle bridge linking minerals and gas sorption capacity.

Additionally, it should be pointed out that samples used for correlating the minerals to microstructure or gas sorption capacity are relatively low rank coals. Their mineral contents are generally lower than middle–high rank coals. This positive correlation is not generalizable to all types of coals. In fact, the positive or negative correlation depends on which of the influences contributes more significantly. In this study, we found a positive influence of mineral matter on microstructure and gas sorption capacity. It is reasonable because mineral content is relative low will make the influence of mineral occurrence and composition to play a more significant role.

4. Conclusions

SEM, EDX, and XRD analyses allowed for the characterization of minerals in coal including morphology, occurrence modes, composition, and content. Low temperature N_2 isotherm analyses displayed the microstructure of coal samples. Methane isotherm analyses revealed the gas sorption capacity of coals. Based on a series of analyses to determine the relationships among minerals, microstructure, and gas sorption capacity, a number of important conclusions can be made and are summarized below:

1. Mineral content was smaller in low rank coals than in middle–high rank coals in this study. In low rank coal, minerals commonly occurred as well as crystallized mineral particles and aggregates infilling in the cell cavities or dispersing on the surface. However, these substances were predominately dispersed on the surface in high rank coals. The group of clay minerals was the main minerals in all kinds of coal. Clay minerals generally made up over 50% of the total with a few samples approaching 90%. The group of carbonate minerals was the second most abundant. Sulfate minerals and quartz were the third most abundant minerals in low rank coals and sulfide minerals were the third most abundant in high rank coals.
2. Mineral occurrence mode has impacts on microstructure and gas sorption capacity. Minerals on the matrix surface or filled in pores and fractures decreased the surface area, furthermore, mineral infillings also decreased the pore volume. However, some interspaces between minerals and the stimulation of new micro-fractures may increase flow network connectivity or even connect some dead end pores to increase surface area and pore volume. The decreased or increased surface area or pore volume will reduce or enhance the gas sorption capacity.
3. Mineral composition has impacts on microstructure and gas sorption capacity. We found that clay mineral content has the strongest positive relation to S_{BET}, total V_{BJH}, and V_L, compared to total mineral and brittle mineral content. The relation of other minerals to S_{BET}, total V_{BJH}, and V_L is weak.
4. Mineral content, mineral occurrence and mineral composition are three controlling factors that together determined the influence of mineral matter on gas sorption capacity. Some factors have the potential for both positive and negative influence. This explains why negative and positive influences of mineral matter on gas sorption capacity have been found. In fact, the magnitude and direction of influence depends on the relative weight of factors. In this study, we found a positive influence of mineral matter on microstructure and gas sorption capacity.

Acknowledgments

The authors acknowledge financial support from the various funding agencies including the National Natural Science Foundation of China (40730422), the Key Project of the National Science & Technology (2011ZX05034-001), the Doctoral Scientific Fund Project of the Ministry of Education of China (20130022110010), State Key Lab of Coal Resources and Safe Mining (SKLCRSM13KFA01) and the China Scholarship Council.

References

ASTM, 2006. Annual book of ASTM Standards. Section five: petroleum products, lubricants, and fossil fuels. Gaseous Fuels Coal and Coke, West Conshohocken, PA, 05.06, 705 pp.
Barrett, E.P., Joyner, L.G., Halenda, P.P., 1951. J. Am. Chem. Soc. 73, 373.
Brunauer, S., Emmett, P.H., Teller, E., 1938. J. Am. Chem. Soc. 62, 1723.
Bustin, R.M., 1997. Importance of fabric and composition on the stress sensitivity of permeability in some coals, northern Sydney basin, Australia: relevance to coalbed methane exploitation. AAPG Bull. 81, 1894–1908.
Bustin, R.M., Clarkson, C.R., 1998. Geological controls on coalbed methane reservoir capacity and gas content. Int. J. Coal Geol. 38, 3–26.
Cai, Y., Liu, D., Yao, Y., Li, J., Qiu, Y., 2011. Geological controls on prediction of coalbed methane of No. 3 coal seam in Southern Qinshui Basin, North China. Int. J. Coal Geol. 88, 101–112.
Carroll, R.E., Pashin, J.C., 2003. Relationship of Sorption Capacity to Coal Quality: CO_2 Sequestration Potential of Coalbed Methane Reservoirs in the Black Warrior Basin. International Coalbed Methane Symposium, Tuscaloosa, Alabama, USA proceedings, paper, 0317.
Chalmers, G.R.L., Bustin, R.M., 2007. The organic matter distribution and methane capacity of the Lower Cretaceous strata of northern Brithish Columbia, Canada. Int. J. Coal Geol. 70, 289–302.
Chen, A., Huang, W., 2004. Selective adsorption of hydrocarbon gases on clays and organic matter. Org. Geochem. 35, 412–423.
Clarkson, C.R., Bustin, R.M., 1996. Variation in micropore capacity and size distribution in coals of the western Canadian sedimentary basin. Fuel 73, 272–277.
Crosdale, P.J., Beamish, B.B., Valix, M., 1998. Coalbed methane sorption related to coal composition. Int. J. Coal Geol. 35, 147–158.
Dai, S., Chou, C., 2007. Occurrence and origin of minerals in a chamosite-bearing coal of late permian age, Zhaotong, Yunnan, China. Am. Mineralogist 92, 1253–1261.
Dai, S., Chou, C., Zhou, Y., Zhao, M., Wang, L., Yang, Z., Cao, H., Ren, D., 2008. Mineralogical and compositional characteristics of Late permian coals from an area of high lung cancer rate in Xuan Wei, Yunnan, China: occurrence and origin of quartz and chamosite. Int. J. Coal Geol. 76, 318–327.
Dai, S., Ren, D., Chou, C., Li, S., Jiang, Y., 2006. Mineralogy and geochemistry of the No. 6 coal (Pennsylvanian) in the Junger Coalfield, ordos Basin, China. Int. J. Coal Geol. 66, 253–270.
Daniels, E.J., Marshak, S., Altaner, S.P., 1996. Use of clay-mineral alteration patterns to define syntectonic permeability of joints (cleat) in Pennsylvanian anthracite coal. Tectonophysics 263, 123–136.
Faiz, M.M., Aziz, N.I., Hutton, A.C., Jones, B.G., 1992. Porosity and gas sorption capacity of some eastern Australian coals in relation to coal rank and composition. In: Symp. Coalbed Methane Res. and Develop., Dept. of Earth Sci., James Cook Univ, vol. 4, pp. 9–20. Townsville.
Gamson, P.D., Beamish, B.B., Johnson, D.P., 1996. Coal microstructure and secondary mineralization: their effect on methane recovery. Geol. Soc. 109 (1), 165–179. London, Special Publications.
Gan, H., Nandi, S.P., Walker, P.L., 1972. Nature of porosity in American coals. Fuel 51, 272–277.
Gray, I., 1987. Reservoir engineering in coal seams: part 1-the physical process of gas storage and movement in coal seams. SPE Res. Eng. 28–34.
Karacan, C.O., Okandan, E., 1999. Heterogeneity effects on the storage and production of gas from coal seams. Houston. In: Proceedings of SPE Annual Technical Conference and Exhibition, pp. 3–6. October, SPE Paper 56551.
Karacan, C.O., Okandan, E., 2001. Adsorption and gas transport in coal microstructure: investigation and evaluation by quantitative X-ray CT imaging. Fuel 80, 509–520.
Koukouzas, N., Ward, C.R., Li, Z., 2010. Mineralogy of lignites and associated strata in the Mavropigi field of the Ptolemais Basin, northern Greece. Int. J. Coal Geol. 81, 182–190.
Langmuir, I., 1918. J. Am. Chem. Soc. 40, 1361.
Laubach, S.E., Marrett, R.A., Olson, J.E., Scott, A.R., 1998. Characteristics and origins of coal cleat: a review. Int. J. Coal Geol. 35, 175–207.
Laxminarayana, C., Crosdale, P.J., 1999. Role of coal type and rank on methane

sorption characteristics of Bowen Basin, Australia coals. Int. J. Coal Geol. 40, 309–325.
Laxminarayana, C., Crosdale, P.J., 2002. Controls on methane sorption capacity of Indian coals. AAPG Bull. 86, 201–212.
Li, Y., Tang, D., Elsworth, D., Xu, H., 2014. Characterization of coalbed methane reservoirs at multiple length scales: a cross-section from southeastern Ordos Basin, China. Energy & Fuels 28, 5587–5595.
Liu, A., Fu, X., Wang, K., An, H., Wang, G., 2013. Investigation of coalbed methane potential in low rank coal reservoirs-free and soluble gas contents. Fuel 112, 14–22.
Liu, B., Huang, W., Ao, W., Zhang, S., Wu, J., Xu, Q., Teng, J., 2014. Occurrence characteristics of minerals and their influences on physical properties of coal reservoirs in Southern Qinshui Basin. Geoscience 28 (3), 645–652 (Chinese with English Abstract).
Liu, D., Yao, Y., Tang, D., Tang, S., Che, Y., Huang, W., 2009. Coal reservoir characteristics and coalbed methane resource assessment in Huainan and Huaibei coalfields, Southern North China. Int. J. Coal Geol. 79, 97–112.
Lv, Y., Tang, D., Xu, H., Luo, H., 2012. Production characteristics and the key factors in high-rank coalbed methane fields: a case study on the Fanzhuang Block, Southern Qinshui Basin, China. Int. J. Coal Geol. 96–97, 93–108.
Ma, X., Song, Y., Liu, S., Jiang, L., Hong, F., 2014. Quantitative research on adsorption capacity evolution of middle-high rank coal reservoirs in geological history: a case study from Hancheng area in Ordos Basin. Acta Pet. Sin. 35 (6), 1080–1086.
Meng, Y., Tang, D., Xu, H., Li, C., Li, L., Meng, S., 2014. Geological controls and coalbed methane production potential evaluation: a case study in Liulin area, eastern Ordos Basin, China. J. Nat. Gas Sci. Eng. 21, 95–111.
Pillalamarry, M., Harpalani, S., Liu, S., 2011. Gas diffusion behavior of coal and its impact on production from coalbed methane reservoirs. Int. J. Coal Geol. 86, 342–348.
Pitman, J.K., Pashin, J.C., Hatch, J.R., Goldhaber, M.B., 2003. Origin of minerals in joint and cleat systems of the Pottsville formation, Black Warrior basin, Alabama: implications for coalbed methane generation and production. AAPG Bull. 87, 713–731.
Rietveld, H.M., 1969. A profile refinement method for nuclear and magnetic structures. J. Appl. Crystallogr. 2, 65–71.
Spears, D.A., Caswell, S.A., 1986. Mineral matter in coals: cleat mineral and their origin in some coals from the English Midlands. Int. J. Coal Geol. 6, 107–125.
Stowell, J.F.W., Laubach, S.E., Olson, J.E., 2001. Effect of modern state of stress on flow-controlling fractures: a misleading paradigm in need of revision. In: Elsworth, D., Tinucci, J.P., Heasley, K.A. (Eds.), Rock Mechanics in the National Interest: U.S. Symposium on Rock Mechanics. Balkema, Washington, DC.: Rotterdam, pp. 691–697.
Su, X., Lin, X., Liu, S., Zhao, M., Song, Y., 2005. Geology of coalbed methane reservoirs in the Southeast Qinshui Basin of China. Int. J. Coal Geol. 62, 197–210.
Tao, S., Wang, Y., Tang, D., Xu, H., Lv, Y., He, W., Li, Y., 2012. Dynamic variation effects of coal permeability during the coalbed methane development process in the Qinshui Basin, China. Int. J. Coal Geol. 93, 16–22.
Taylor, J.C., 1991. Computer programs for standardless quantitative analysis of minerals using the full powder diffraction profile. Powder Diffr. 6, 2–9.
Wang, X., Dai, S., Chou, C., Zhang, M., Wang, J., Song, X., Wang, W., Jiang, Y., Zhou, Y., Ren, D., 2012. Mineralogy and geochemistry of late permian coals from the Taoshuping Mine, Yunnan Province, China: evidences for the sources of minerals. Int. J. Coal Geol. 96–97, 49–59.
Ward, C.R., 2002. Analysis and significance of mineral matter in coal seams. Int. J. Coal Geol. 50, 135–168.
Ward, C.R., Matulis, C.E., Taylor, J.C., Dale, L.S., 2001. Quantification of mineral matter in Argonne premium coals using interactive rietveld-based X-ray diffraction. Int. J. Coal Geol. 46, 67–82.
Ward, C.R., Taylor, J.C., Cohen, D.R., 1999. Quantitative mineralogy of sandstones by X-ray diffractometry and normative analysis. J. Sediment. Res. 69, 1050–1062.
Xu, H., Tang, D., Liu, D., Tang, S., Yang, F., Chen, X., He, W., Deng, C., 2012. Study on coalbed methane accumulation characteristics and favorable areas in the Binchang area, southwestern Ordos Basin, China. Int. J. Coal Geol. 95, 1–11.
Yao, Y., Liu, D., Tang, D., Tang, S., Huang, W., 2008. Fractal characterization of adsorption-pores of coals from North China: an investigation on CH_4 adsorption capacity of coals. Int. J. Coal Geol. 73, 27–42.
Yee, D., Seidle, J.P., Hanson, W.B., 1993. Gas sorption on coal and measurement of gas content. In: Law, B.E., Rice, D.D. (Eds.), Hydrocarbons from Coal. AAPG Studies in Geology, vol. 38, pp. 203–218.
Zhang, S., Tang, S., Tang, D., Pan, Z., Yang, F., 2010. The characteristics of coal reservoir pores and coal facies in Liulin district, Hedong coal field of China. Int. J. Coal Geol. 81, 117–127.